

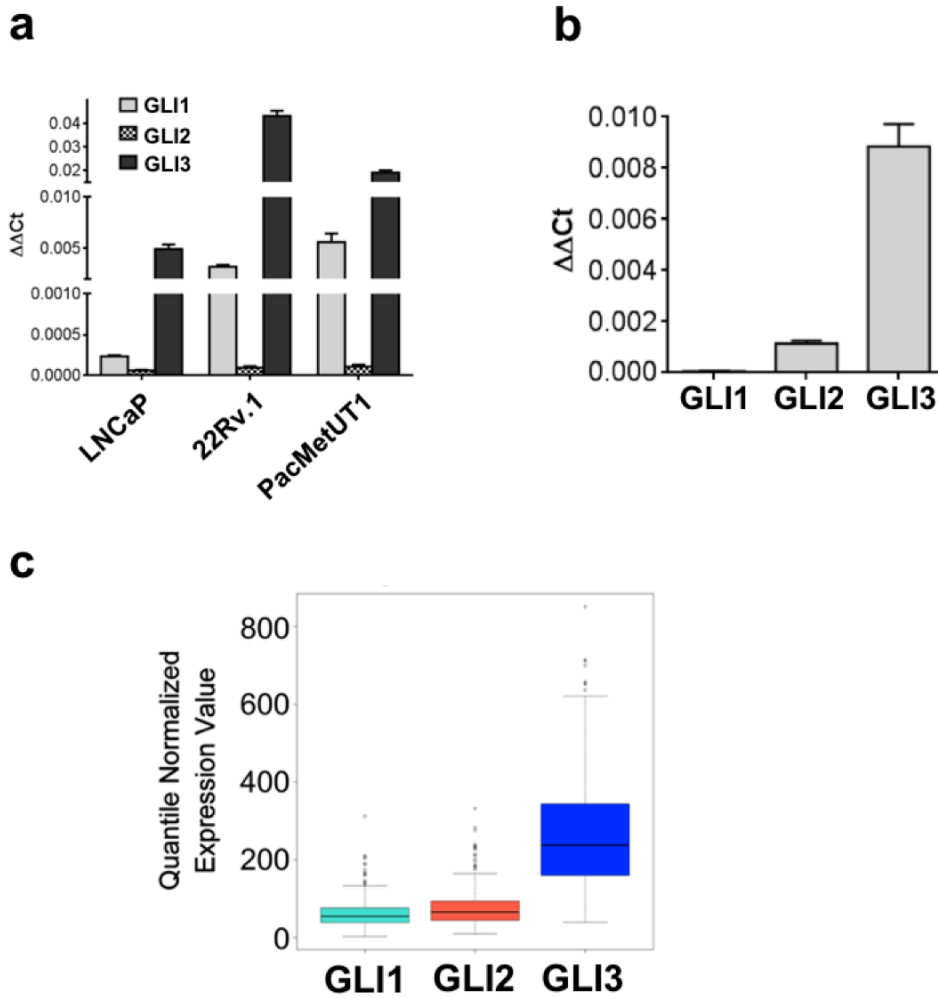
Supplementary Data

**Includes:
Supplementary Figures
Supplementary Materials and Methods**

GLI3 is stabilized by SPOP mutations and functionally crosstalks with androgen receptor to drive prostate cancer progression

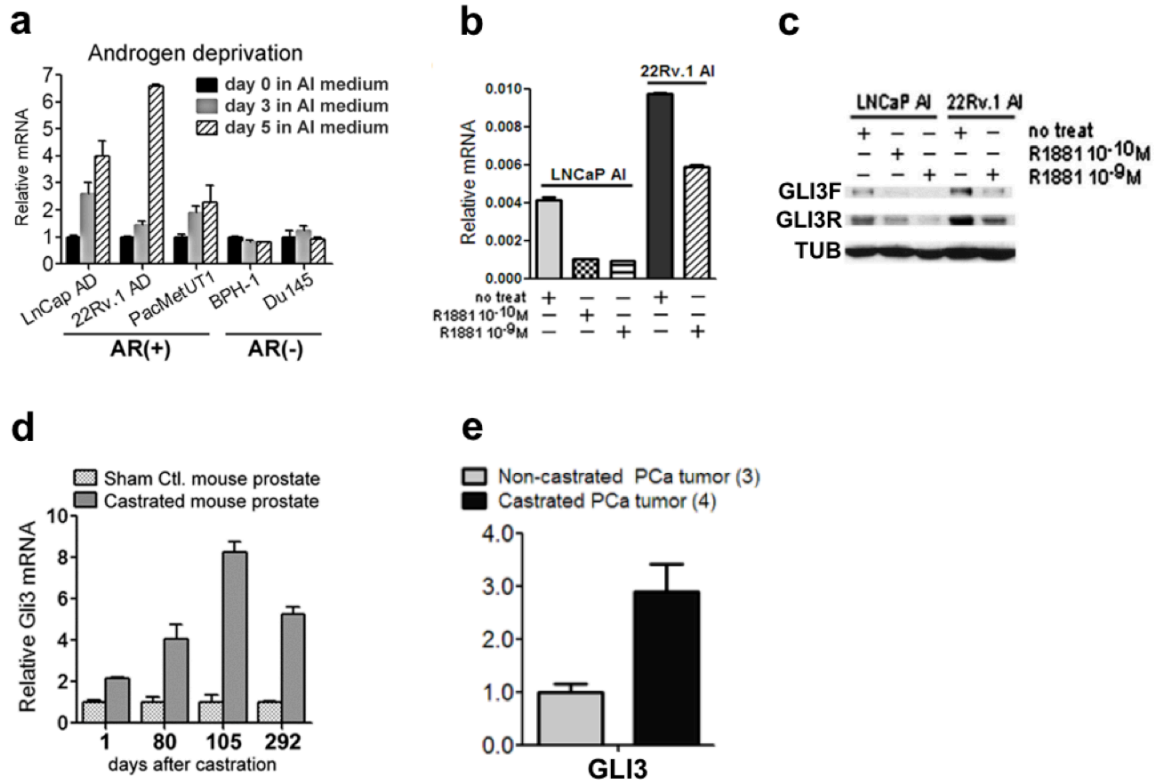
Marieke Burlison, Janice J. Deng, Tai Qin, Thu Minh Duong, Yuqian Yan, Xiang Gu, Debodipta Das, Acarizia Easley, Michael A. Liss, P. Renee Yew, Roble Bedolla, Addanki Pratap Kumar, Tim Hui-Ming Huang, Yi Zou, Yidong Chen, Chun-Liang Chen, Haojie Huang, Lu-Zhe Sun and Thomas G. Boyer

Supplementary Figure 1



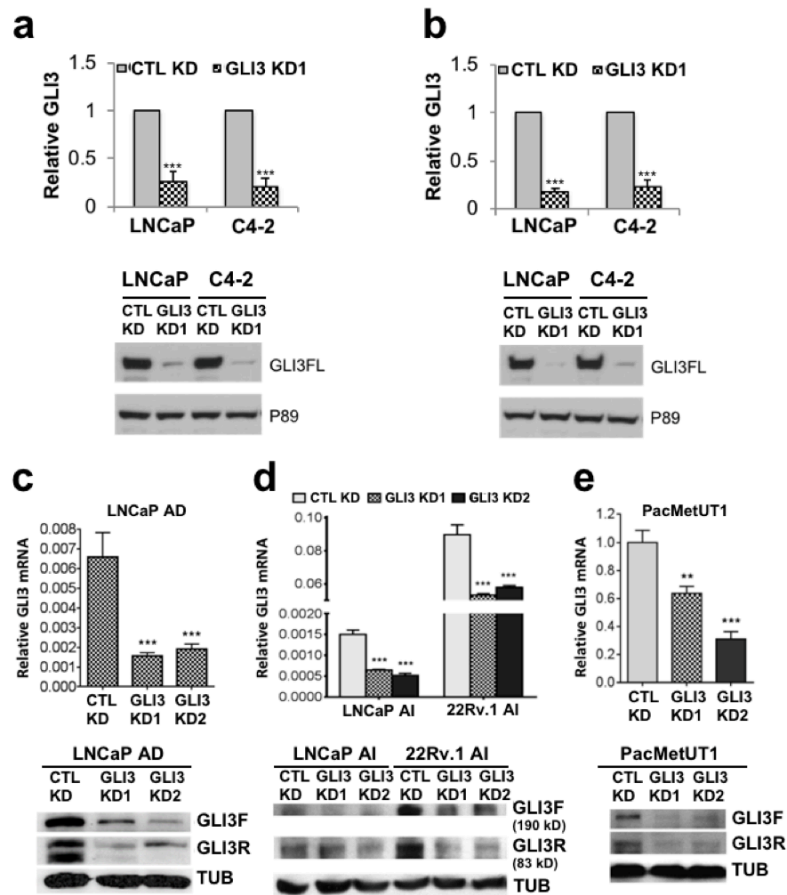
Supplementary Figure 1. GLI3 mRNA is expressed at higher levels than GLI1 or GLI2 mRNAs in human prostate cancer. GLI1, GLI2, and GLI3 mRNAs were measured with RT-qPCR in three human prostate cancer cell lines (**a**) and CWR22 xenograft tumors (**b**), and with next generation RNA sequencing in human prostate cancer tissues from TCGA database (**c**).

Supplementary Figure 2



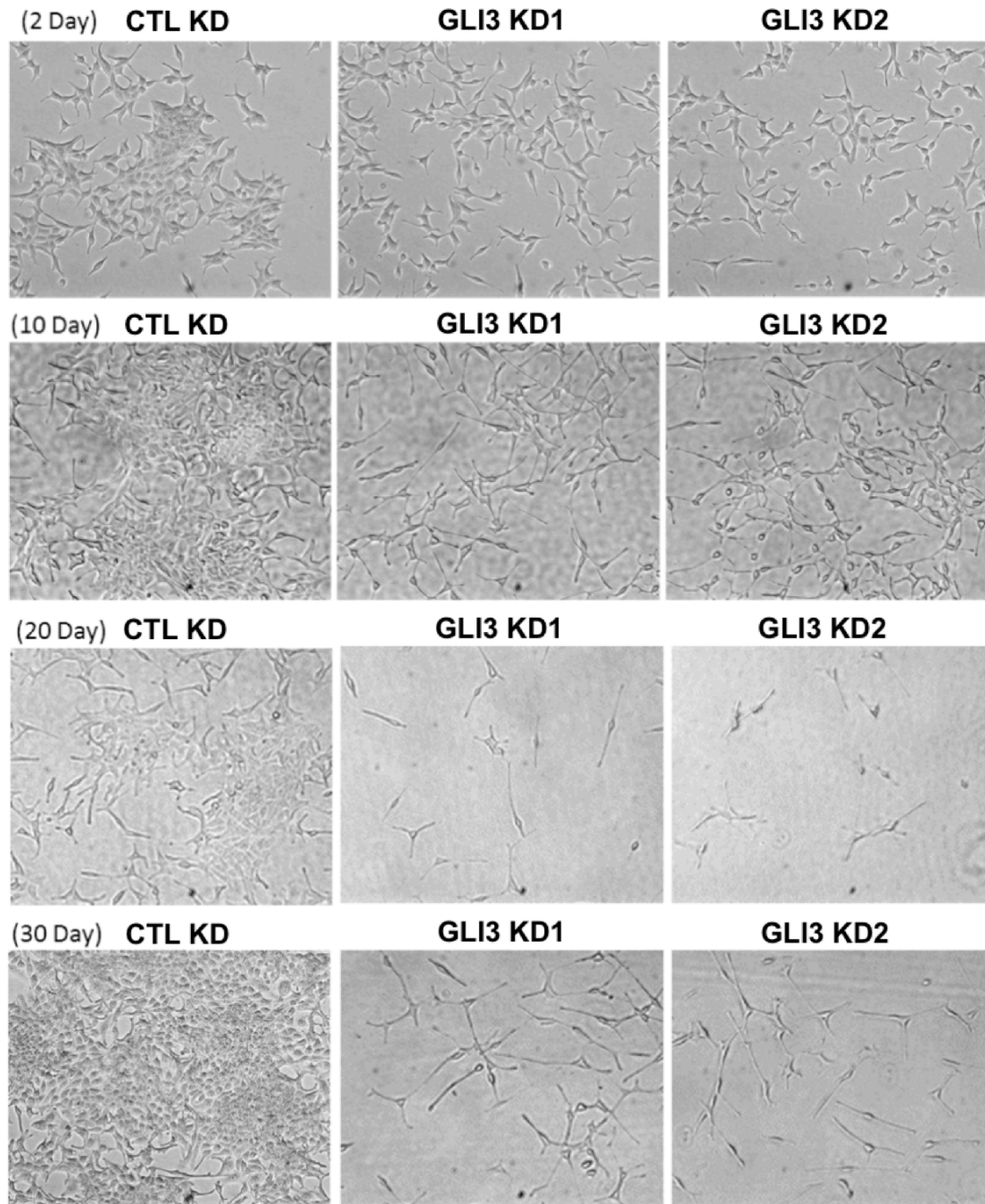
Supplementary Figure 2. GLI3 is negatively regulated by androgen. **a** Transient androgen deprivation triggers upregulation of GLI3 expression in androgen receptor-positive [AR(+)] but not androgen receptor-negative [AR(-)] prostate cancer cells. AR(+) and AR(-) prostate cancer cells were transitioned from androgen replete to androgen-depleted [androgen independent (AI)] medium and harvested for RT-qPCR immediately before transition (day 0) and at days 3 and 5 following transition. GLI3 mRNA levels were normalized to β -actin and expressed relative to the level of GLI3 mRNA at day 0. **b, c** Synthetic androgen R1881 downregulates GLI3 mRNA and protein levels in AR(+) prostate cancer cells. LNCaP and 22Rv.1 cells growing in AI medium were treated without (no treat) or with R1881 at the indicated concentrations for 2 days prior to analysis by RT-qPCR (**b**) or immunoblot analysis (**c**). GLI3 mRNA levels in each cell line were normalized to β -actin and expressed relative to GLI3 (no treat). Whole cell lysates were processed for immunoblot analysis using antibodies specific for the GLI3 N-terminus [recognizing both full-length activator (GLI3F) and truncated repressor (GLI3R) forms] or tubulin (TUB) as indicated. **d, e** GLI3 expression is upregulated *in vivo* after castration in normal mouse prostate and in mice bearing prostate tumor xenografts. (**d**) Prostates were harvested from uncastrated (sham Ct) or castrated male BALB/c mice at the indicated times and processed for RT-qPCR. Gli3 mRNA levels were normalized to β -actin and expressed relative to the level of mouse Gli3 mRNA in sham control mouse prostate. (**e**) Male NSG mice bearing CWR22 prostate tumor xenografts were sham castrated (non-castrated) or castrated and 14 days thereafter euthanized for analysis of GLI3 mRNA expression by RT-qPCR in xenograft tissue. GLI3 mRNA levels were normalized to β -actin and expressed relative to the level of Gli3 mRNA in tumor xenografts of non-castrated mice.

Supplementary Figure 3



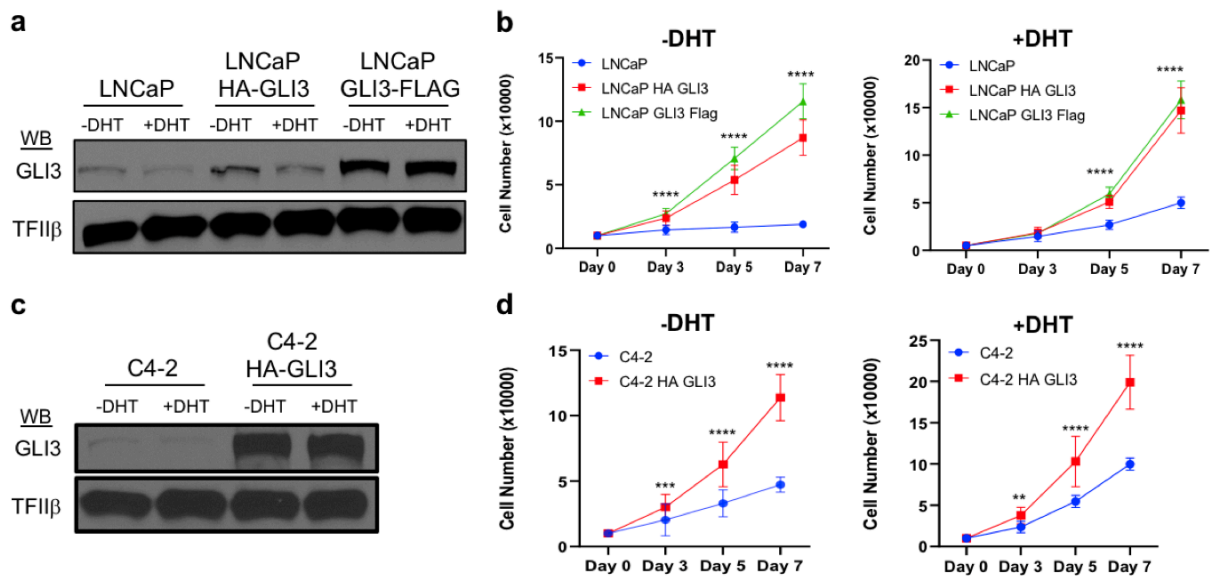
Supplementary Figure 3. Validation of GLI3 knockdown in human prostate cancer cells. **a, b** LNCaP or C4-2 cells in androgen replete medium were transduced with lentiviruses expressing control (CTL) or GLI3-specific (GLI3 KD1) shRNAs, and cultured for 3 days under puromycin selection prior to transition into androgen depleted medium. Control and GLI3 knockdown cells were processed by RT-qPCR (**a** and **b**, *top panels*) and immunoblot (**a** and **b**, *bottom panels*) to confirm GLI3 knockdown at both mRNA and protein levels. Panel **a** and **b** correspond, respectively, to cells used for analysis of GLI3 target gene expression (Fig. 1a and b) and proliferation (Fig. 1c and d). **c-e** LNCaPAD, LNCaP AI, 22Rv1, or PacMetUT1 cells in androgen-replete medium were transduced with lentiviruses expressing control (CTL) or two different GLI3-specific (GLI3 KD1, GLI2 KD3) shRNAs prior to analysis of proliferation, colony formation, and migration (see Fig 1e-n). Cells were also harvested for isolation of RNA and protein for analysis by RT-qPCR (*top panels*) and immunoblot (*bottom panels*), respectively. GLI3 mRNA levels were normalized to GAPDH (**a** and **b**) or β -actin (**c-e**) and expressed relative to the level of GLI3 mRNA in control knockdown cells. Data are the mean \pm SEM of 3 experiments performed in triplicate. Asterisks denote significant differences relative to control knockdown (Student's *t*-test: ** $p < 0.01$; *** $p < 0.001$). GLI3 protein was detected with an anti-GLI3 antibody. Both GLI3 full-length activator (GLI3F) and truncated repressor (GLI3R) forms are indicated. The p89 subunit of TFIIF (**a** and **b**) or Tubulin (TUB; **c-e**) were used as internal loading controls.

Supplementary Figure 4



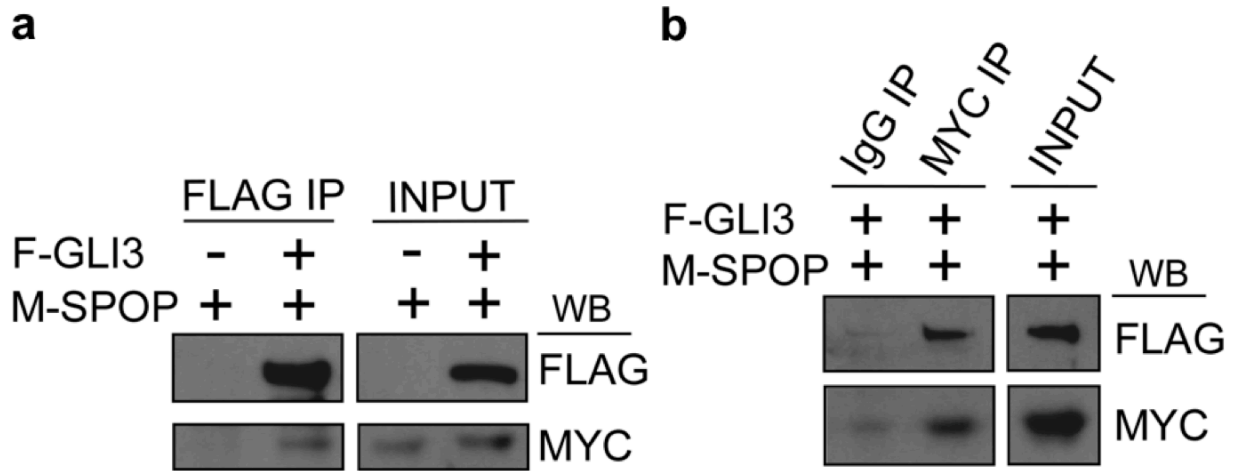
Supplementary Figure 4. GLI3 knockdown blocks acquisition of androgen-independent prostate cancer cell growth. Stable LNCaP/control (CTL KD) and two independent LNCaP/GLI3 (GLI3 KD1, GLI3 KD2) shRNA-expressing cell lines were grown in androgen depleted medium for 2, 10, 20, and 30 days. Cell cultures were monitored by phase contrast microscopy showing suppressed cell survival by GLI3 KD.

Supplementary Figure 5



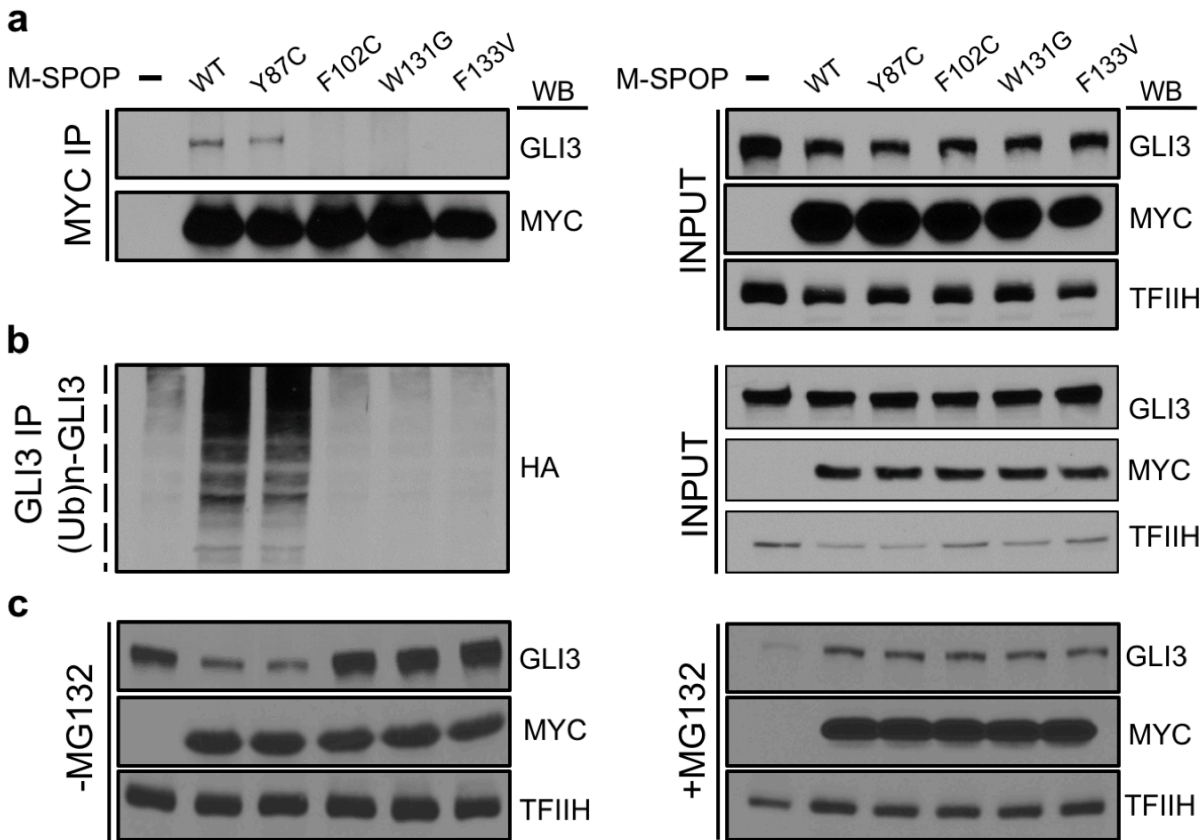
Supplementary Figure 5. Ectopic GLI3 promotes androgen-dependent and androgen-independent prostate cancer cell growth. **a, b** Parental LNCaP cells or LNCaP cell lines stably expressing HA-GLI3 or GLI3-FLAG epitope-tagged derivatives as indicated were cultured under androgen-deplete (-DHT) or androgen-replete (+DHT) conditions. **(a)** Whole cell lysates were directly processed by western blot (WB) using antibodies specific for GLI3 and TFII β (internal loading control). **(b)** Cells were seeded in replicate wells on Day 0, and proliferation was monitored by viable cell counting (using Trypan Blue) on days 3, 5, and 7 thereafter. Data are the mean \pm SEM of 4 experiments in triplicate. Asterisks denote statistically significant differences vs LNCaP cells (Two-way ANOVA: $p^{****} < 0.0001$). **c, d** Parental C4-2 cells or C4-2 cells stably expressing HA-GLI3 as indicated were cultured under androgen-deplete (-DHT) or androgen-replete (+DHT) conditions. **(c)** Whole cell lysates were directly processed by WB using antibodies specific for GLI3 and TFII β . **(d)** Cells were seeded in replicate wells on Day 0, and proliferation was monitored by viable cell counting (using Trypan Blue) on days 3, 5, and 7 thereafter. Data are the mean \pm SEM of 3 experiments in triplicate. Asterisks denote statistically significant differences vs C4-2 cells (Student's t-test: $p^{**} < 0.01$; $p^{***} < 0.001$; $p^{****} < 0.0001$).

Supplementary Figure 6



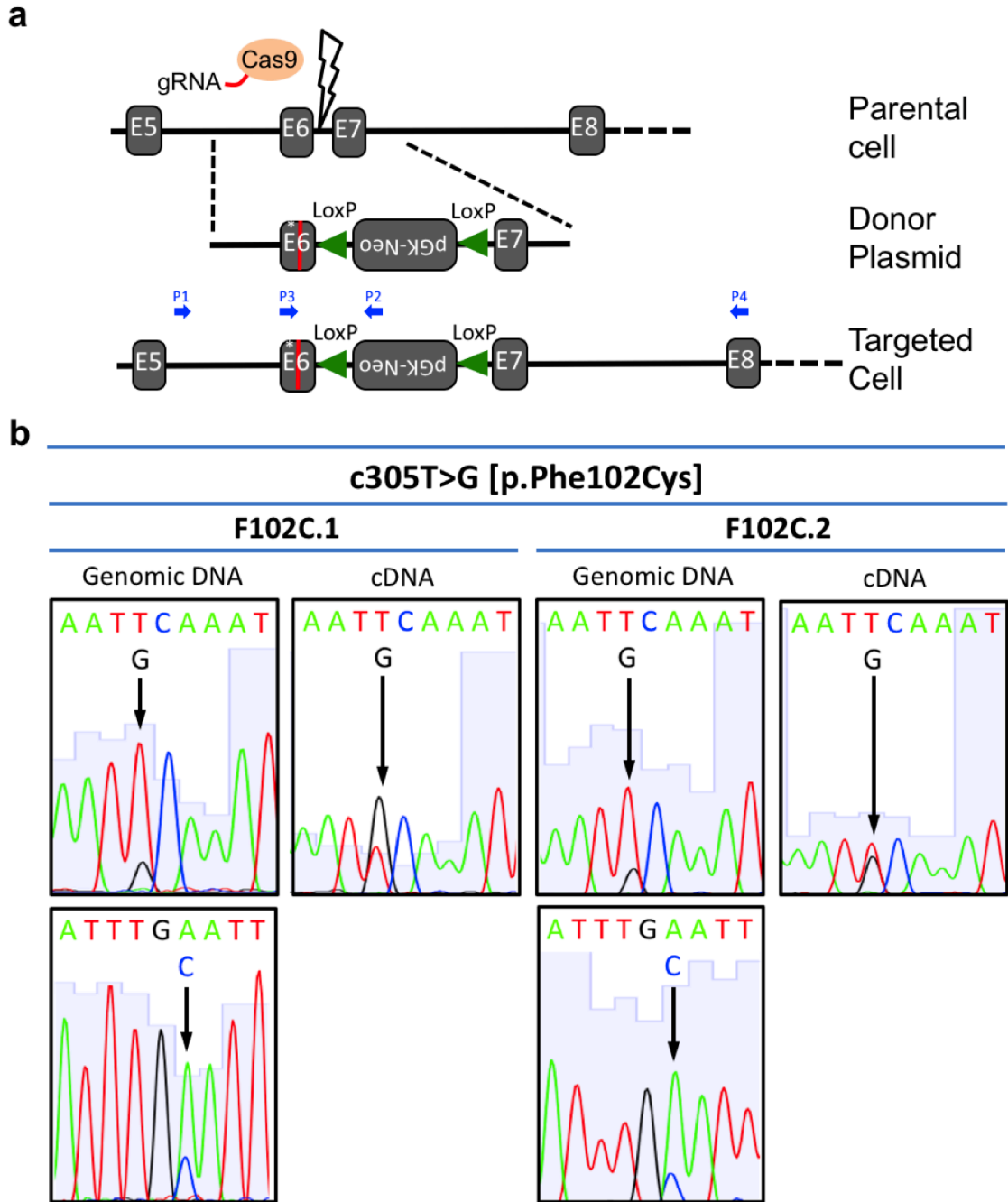
Supplementary Figure 6. Ectopically expressed GLI3 and SPOP proteins interact in mammalian cells. **a, b** Whole cell lysates from HEK293T cells transfected with pCMV:MYC-SPOP (M-SPOP; +), pACT:FLAG-GLI3 (F-GLI3; +), or pACT:FLAG empty vector (F-GLI3; -) as indicated were subjected to co-immunoprecipitation analysis using anti-FLAG agarose (**a**) or IgG or anti-MYC epitope antibodies (**b**). Immunoprecipitates were processed by immunoblot analysis using antibodies specific for the FLAG or MYC epitopes as indicated.

Supplementary Figure 7



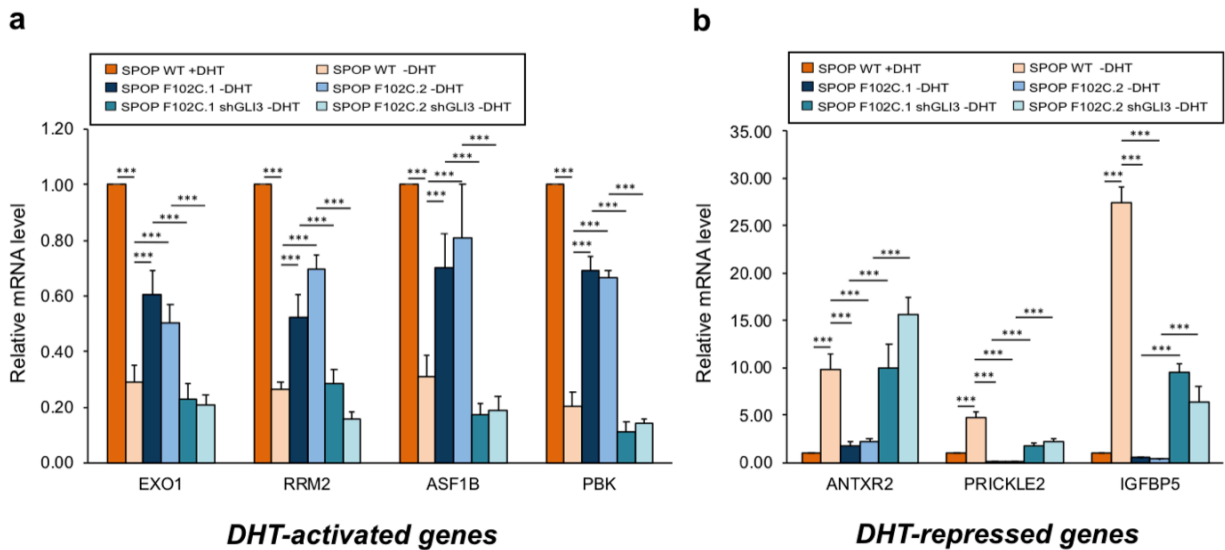
Supplementary Figure 7. GLI3 is targeted for proteasomal degradation by WT but not oncogenic mutant SPOP in androgen-independent and AR-negative PC-3 prostate cancer cells. **a** and **b** PC-3 cells cultured under androgen-deplete conditions were transfected without or with Myc-tagged SPOP (M-SPOP; WT or mutant as indicated); at 24 hrs post-transfection, cells were treated with MG132 (15 μ M; 18 hrs). In **(b)**, cells were also transfected with HA-tagged ubiquitin (Ub). Transfected whole cell lysates were subjected to IP with MYC epitope-specific antibodies **(a)** or GLI3-specific antibodies **(b)** and processed by WB using antibodies specific for GLI3, Myc or HA epitopes, or TFIIH (p89 subunit) as a loading control. INPUT, 10% of lysate used in IP. **c** PC-3 cells transfected without or with Myc-tagged SPOP (M-SPOP; WT or mutant as indicated) were treated at 24 hrs post-transfection without or with MG132 (15 μ M; 18 hrs). Transfected whole cell lysates were directly processed by WB using antibodies specific for GLI3, the Myc epitope, or TFIIH (p89).

Supplementary Figure 8



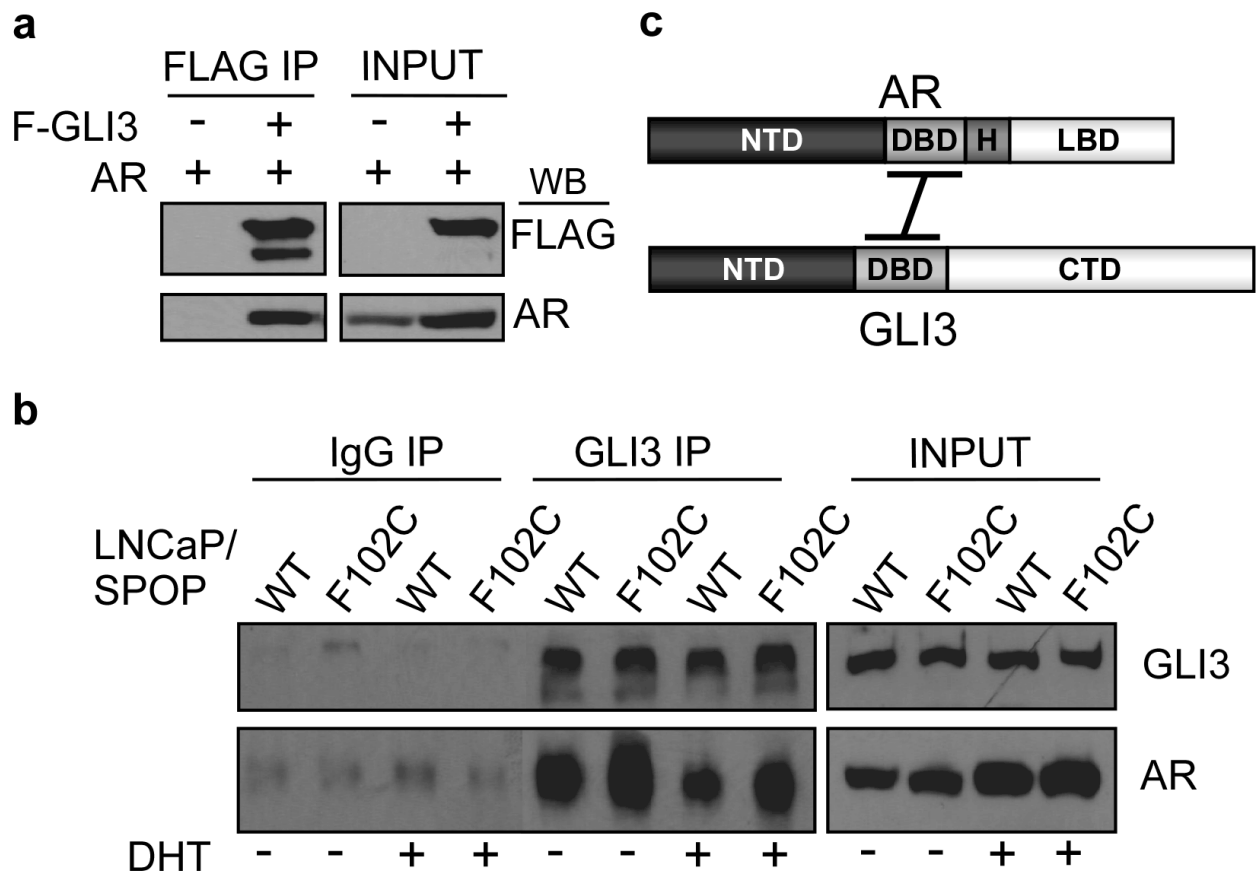
Supplementary Figure 8. Validation of SPOP mutant F102C knock-in cell lines. **a** Schematic diagram of knock-in strategy. Red line represents missense mutation (c.305 T>G, p.F102C), green arrowheads indicate loxP sites, and blue arrows indicate primers used for subsequent genotyping. **b** Sequence chromatogram of targeted mutations. Genomic DNA or cDNA derived from two independent clonal cell lines (F102C.1 and F102C.2 as indicated) following gene targeting and selection was subjected to Sanger sequencing using primers indicated in A (P1/P2 for genomic DNA; P3/P4 for cDNA).

Supplementary Figure 9



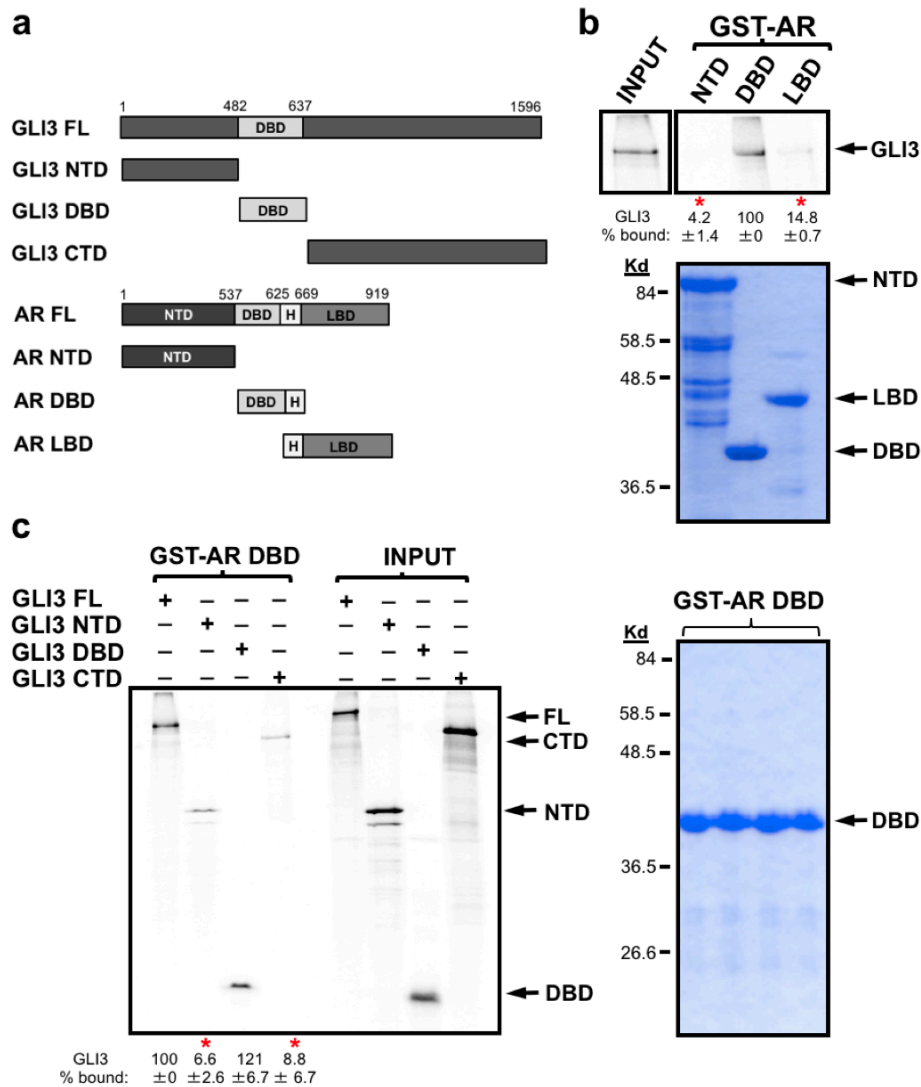
Supplementary Figure 9. Validation of RNA-sequencing data. SPOP WT and F102C mutant LNCaP cells (clones F102C.1 and F102C.2), cultured in androgen replete or androgen deplete medium (+/- DHT) as indicated, were transduced without or with GLI3-specific (shGLI3) shRNA-expressing lentivirus prior to harvest and isolation of RNA. mRNA levels of 7 randomly selected genes from among the 184 overlapping SPOP, AR, and GLI3 regulated genes identified through RNA-seq (Fig. 4H; Table S4), including 4 DHT-activated (**a**) and 3 DHT-repressed (**b**) genes were quantified by RT-qPCR, normalized to GAPDH mRNA, and expressed relative to their levels in SPOP WT LNCaP cells (+DHT). Data are mean \pm SEM of 3 experiments in duplicate. Asterisks denote significant differences (Student's *t*-test: *** $p < 0.001$). Note that expression levels of these 7 genes in androgen depleted (-DHT) SPOP mutant cells (dark and light blue bars) approaches their corresponding expression levels in androgen replete (+DHT) WT SPOP cells (dark orange bars), indicating partial restoration of AR signaling in the former. Notably, GLI3 knockdown reverses this effect, diminishing restored androgen signaling in SPOP mutant cells (dark and light turquoise bars).

Supplementary Figure 10



Supplementary Figure 10. GLI3 and AR interact directly through their DBDs. **a** Whole cell lysates from HEK293T cells transfected without or with FLAG-tagged GLI3 (F-GLI3) and AR were immunoprecipitated (IP) with FLAG-specific antibodies, resolved by SDS-PAGE, and processed by WB with antibodies specific for the FLAG epitope and AR. **b** SPOP WT and F102C mutant LNCaP cells cultured in the absence (-) or presence (+) of DHT were treated with MG132 (20 μ M) for 18 hrs prior to IP of whole cell lysates with GLI3-specific antibody or isotype-matched IgG. IPs were processed by WB using antibodies specific for GLI3 and AR. INPUT, 10% of lysate used in IP. **c** Summary of in vitro binding assays with recombinant GLI3 and AR protein derivatives (data shown in Supplementary Figure 11).

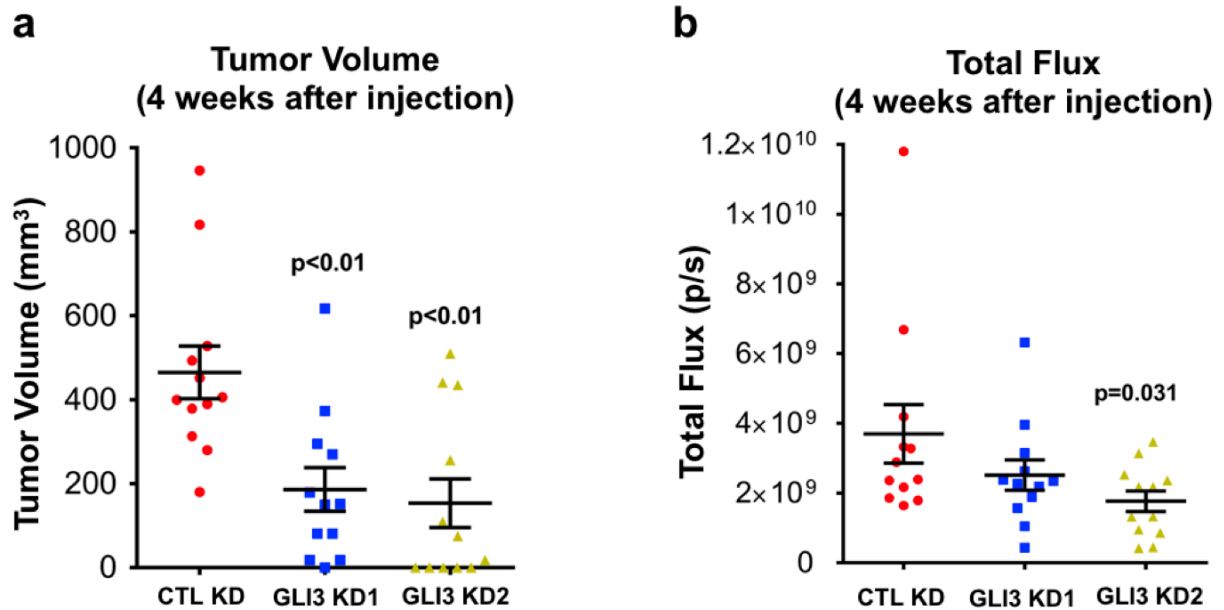
Supplementary Figure 11



Supplementary Figure 11. GLI3 and AR interact through their respective DNA-binding domains.

a Diagram of full-length (FL) GLI3 and AR proteins and their corresponding truncation derivatives used for in vitro binding reactions. Numbers refer to amino acid coordinates. Abbreviations: NTD, N-terminal domain; DBD, DNA-binding domain; CTD, C-terminal domain; LBD, ligand-binding domain; H, Hinge region. **b, c** Recombinant full-length GLI3 (**b** and **c**) or its specified truncation derivatives (**c**) were expressed and radiolabeled with [³⁵S]methionine by translation in vitro prior to incubation with the indicated glutathione-Sepharose-immobilized GST-AR derivatives. Bound proteins were eluted with Laemmli sample buffer, resolved by SDS-PAGE, and visualized by phosphorimager analysis. Coomassie blue stained gels show GST-AR derivatives used in binding reactions. The amount of each radiolabeled GLI3 derivative retained by each GST-AR derivative (% bound) was quantified and is expressed relative to the level of full-length GLI3 bound to GST-AR DBD, which was arbitrarily assigned a value of 100%. Data represent the mean ± SEM of 3 independent binding experiments. Asterisks denotes statistically significant GLI3 binding differences relative to the level of full-length GLI3 to GST-AR DBD (Student's *t* test, **p* < 0.05).

Supplementary Figure 12



Supplementary Figure 12. GLI3 knockdown suppresses androgen-dependent prostate tumor growth in vivo. Subcutaneous tumors were generated by injection of stable Luc-GFP-expressing LNCaP/control (CTL KD) and two independent LNCaP/GLI3 (GLI3 KD1, GLI3 KD2) shRNA-expressing cell lines into the flanks of NOD scid gamma (NSGTM) mice. Four weeks following cell injections, tumor burden was quantified by volume measurement (a) or bioluminescence imaging (b). Volume measurements were made by a caliper, while bioluminescence imaging was performed by determination of total photon flux. Bars represent the mean ± SEM from twelve single tumors. Note that GLI3 knockdown inhibits LNCaP xenograft tumor growth by tumor volume and photon flux.

Supplementary Materials and Methods

Quantitative real-time PCR. For figures S1-S3, RNA was isolated from prostate cancer cell lines using RNA Mini Spin Column of EnzyMax LLC (Lexington, KY). Extracted RNA was shredded by EZshredder column of EnzyMax LLC (Lexington, KY) to remove genomic DNA contamination. Total RNA (2 ug) was reverse-transcribed into cDNA using random primers and M-MLV reverse transcriptase from Invitrogen in Life Technology (Grand Island, NY). Quantitative real-time PCR (qRT-PCR) was performed using Power SYBR Green PCR Mix from ABI, Applied Biosystems in Life Technologies. Primer pair specificity was determined by generation of a single peak for dissociation curve (melting curve) at the end of RT-PCR cycling program. β -actin, OAZ1 and RPL27 were used for endogenous gene controls. All primers used in this study were designed by Primer Blast of NCBI and synthesized by Integrated DNA Technologies (Coralville, IA). For Figs. 1, 4, and Supplementary Figs. 3a, 3b, and 9, cells were seeded at 4×10^5 cells in 60 mM dishes in androgen deprived or androgen replete media, split 1:2 or 1:6 respectively, on day 5 and harvested for RNA using Trizol reagent on day 10. GLI3 knockdown cells were infected with GLI3 KD1 shRNA-expressing lentivirus or empty pLKO.1 vector and selected with puromycin (3 ug/ml) prior to seeding. Cyclopamine (or DMSO) was added 24 hours prior to RNA harvest for all cyclopamine-treated cells. RNA was reverse transcribed using the ImProm-II Reverse Transcription System (Promega) following standard procedures and used in quantitative reverse transcription-PCR. Primer pair specificity was determined by generation of a single peak for dissociation curve (melting curve) at the end of RT-PCR cycling program. β -actin and GAPDH were used for endogenous gene controls. Primers used for quantitative real-time PCR are listed in Supplementary Table S7.

Cell Proliferation Assays. For MTT assay, cells were plated in a 96-well plate at 1,000-2,000 cells per well in triplicates. After every consecutive day for 6 days, 3-(4,5-Dimethylthiazol-2-yl)-2,5-diphenyltetrazoliumbromide (MTT) from Sigma-Aldrich ((St. Luis, MO) solution (2 mg/ml) was added and incubated for 2 hr in 37°C incubator. 100 µl DMSO was added into each well after the medium was removed, and the plate was gently shaken on a shaker for 10 minutes. The blue colored formazon product was quantified at 595 nm wave length with a Microplate Reader of Bio Tek Instrument (Winooski, VT). For proliferation (cell counting) assays, 2,500 cells were plated in individual 24-well plate wells in triplicate. Cells were trypsonized and counted with a hemocytometer on indicated dates. For determination of cell growth by IncuCyte Zoom analysis, cells were seeded at 5,000 cells/well in androgen replete or 2,000 cells/well in androgen deprived medium in 96-well plates in triplicate and scanned every 3 hours by an IncuCyte ZOOM system. Growth rate was calculated by dividing cell confluence value at each time point by the initial confluence value. Results are the mean of three independent experiments.

Soft Agar and Colony Formation Assays. Cells (2×10^3 - 4×10^3) in 0.5 ml of 0.4% low melting agarose with culture medium were poured on the top of 0.5 ml of 0.8% hardened agar layer in 24-well plates and allowed to solidify. The cells were grown at 37°C in a 5% CO₂ humidified incubator for 10-12 days. The colonies were then stained with 0.5 ml/well of 1 mg/ml INT (p-Iodonitrotetrazolium violet, Sigma) staining solution overnight in an incubator. The plates were scanned and the number visible colonies were counted. For colony formation assays, cells were seeded at 500 cells/well in 6-well plates in androgen deprived media. Media was replaced every

3 days and cells were stained with crystal violet on day 15. For both assays, cells were infected with Control, GLI3 or AR-specific shRNA-expressing lentiviruses and selected with puromycin (3 $\mu\text{g/ml}$) prior to seeding. Over the course of the assay, cells were kept under 2 $\mu\text{g/ml}$ puromycin selection. Cyclopamine or DMSO was added at the time of seeding and replaced fresh every three days. For lawn formation assays, cells were seeded at 1×10^4 cells in 60 mM dishes in androgen deprived media. Media was replaced every three days and images captured at 2, 10, 20 and 30 days. At day 30 cells were rinsed twice in PBS and stained for 30 seconds with crystal violet.

Cell Migration assay. Cells were seeded at 40,000 to 60,000 cells/well in serum-free media into 8- μm pore-size inserts from BD Biosciences (San Jose, CA) in 24-well plates. The bottom chamber contained media with 10% serum to create a chemo-attractive gradient. After 18 h, the cells that did not migrate across the membrane were removed with a cotton swab and the migrated cells through the membrane were fixed and stained with Hema 3 Staining kit (Thermo Fisher Scientific, Waltham, MA,). Stained cells were counted under a microscope with 100X magnification.

Immunoprecipitation and GST pulldown assays. 293T, LNCaP, or PC-3 cells were transfected as described above, harvested at indicated timepoints, and whole cell extracts prepared with lysis buffer (0.42M NaCl, 20mM HEPES, 20% glycerol, 0.2mM EDTA) with a cocktail of protease inhibitor. Whole cell extracts were incubated overnight at 4°C with 5 μg of indicated antibodies. Following addition of protein A-sepharose (for rabbit antibodies) or protein G-agarose (for mouse antibodies) and incubation for 4 hours at 4°C, immune complexes were washed 5 times at 4°C

with 0.3M NaCl buffer. Immunoprecipitated proteins were subsequently eluted with Laemmli sample buffer, resolved by SDS-10% PAGE, and processed by immunoblot analysis.

GST pulldown assays. GST-SPOP and GST-AR derivatives were induced in *E. coli* strain BL21 CodonPlus (Stratagene) with 0.5 mM IPTG for 2 ½ hours at 30°C and soluble lysates were prepared in Lysis 250 buffer (50 mM Tris-HCl, 250 mM NaCl, 5 mM EDTA, 0.1% NP-40) supplemented with protease inhibitors. Resuspended cells were subjected to one freeze-thaw cycle followed by sonication and clarification by centrifugation at 35,000 X g for 30 minutes at 4°C. For GST pulldown assay, normalized amounts of GST derivatives were immobilized on glutathionine-Sepharose beads (GE Healthcare Life Sciences) for 1 hour at 4°C and washed five times with Lysis 250 buffer containing 0.2% NP-40. Bead-immobilized GST derivatives were resuspended in 0.2M KCl D buffer (20 mM HEPES, pH 7.9, 0.2 mM EDTA, 20% glycerol) containing 0.1% NP-40 and subsequently incubated with radiolabeled GLI3 derivatives for 2 hours at 4°C. GLI3 derivatives were expressed and radiolabeled with [35S]-methionine by *in vitro* translation (TNTSP6/T7 quick coupled transcription/translation system, Promega Corp.). After incubation, beads were washed five times with 0.2M KCl D buffer and eluted in Laemmli sample buffer. Samples were resolved by SDS-12% polyacrylamide gel electrophoresis and analyzed by Coomassie brilliant blue staining followed by Phosphor Imager analysis.

Animal studies. For orthotopic xenograft tumor model studies, PacMetUT1 Gli3 shR and control cells (5×10^6) in 50 µl basic medium, mixed with equal volume of Matrigel (BD Biosciences, San Jose, CA), were injected into ventral prostate glands of 6-week-old male nude mice (n=10 per

group, Harlan Inc., Frederick, MD). For subcutaneous xenograft tumor studies, LNCaP Gli3 shR and control cells (5×10^6) in 50 μ l basic medium were mixed with an equal volume of Matrigel, and were subcutaneously implanted on both sides of the lower back of 6-week-old male NSG mice (NOD.Cg-Prkdc^{Scid}IL2rg^{tm1Wjl}/SzJ, Stock No. 005557, The Jackson Laboratory, Sacramento, CA). Each group had 6 mice. Mice were monitored daily for adverse effects. PacMetUT1 orthotopic tumor growth was monitored with bioluminescence imaging with a Xenogen IVIS-Spectrum imaging system (Xenogen Corporation, Alameda, CA) weekly after tumor cell inoculation. One week after inoculation, the mice were subjected to surgical castration. LNCaP subcutaneous tumor growth was monitored weekly with the Xenogen IVIS system. The tumor volume was measured with a caliper and determined in cubic millimeters using the formula $V = (L \times W^2) / 2$, where L is the length and W is the width of a tumor. When tumor volume reached about 300 to 500 mm³, LNCaP mice were castrated surgically. On Day 50 after injection of the PacMetUT1 cells in the nude mice and on Day 57 after castration of the NSG mice with subcutaneous LNCaP tumors, the mice were euthanized and the tumors were excised and individually weighed. Tissues from liver, lung, bone, and kidney were analyzed for metastases under fluorescence microscopy by searching for the presence of green fluorescent protein (GFP)-expressing cells. The number of lung metastatic tumor cell colonies was counted in nude mice.